Radiation-Hard Optical Fiber Benchmark Testing for the LUCID-3 Detector

Cole Morrison

Supervised by Federico Lasagni Manghi and Antonio Sbrizzi

Abstract

The LUCID detector is one of the key luminosity detectors in the ATLAS experiment. Currently, it relies on photomultiplier tubes placed 17 meters from the interaction point, leading to significant radiation damage over time. With the upcoming long shutdown of the Large Hadron Collider in 2026 and the transition to high-luminosity conditions, a major upgrade to the LUCID detector is planned. The upgraded system will utilize multiple sub-detectors. The sub-detector of interest to this report will use radiation-resistant optical fibers which generate and transport Cherenkov light away from the interaction region, protecting sensitive electronics.

This project involved providing benchmark measurements for various optical fibers across a range of wavelengths, prior to irradiation. Eleven fibers of five types were tested, with transmission of light evaluated across ultraviolet, blue, green, and red wavelengths.

The results showed clear differences in transmission efficiency among fibers. This work provides essential baseline data for comparison with post-irradiation results and supports informed fiber selection for the LUCID upgrade.

Geneva, Switzerland

August 12, 2025

Contents

1 Introduction

The ATLAS detector is the largest particle detector within the LHC . It contains numerous sub-detectors that work together to track particles, identify decay products, and measure energy deposits from collisions. One of these is the LUCID detector, which plays a key role in measuring luminosity.

In its current configuration, the LUCID detector uses photomultiplier tubes mounted directly around the beam pipe, 17 meters from the interaction point.

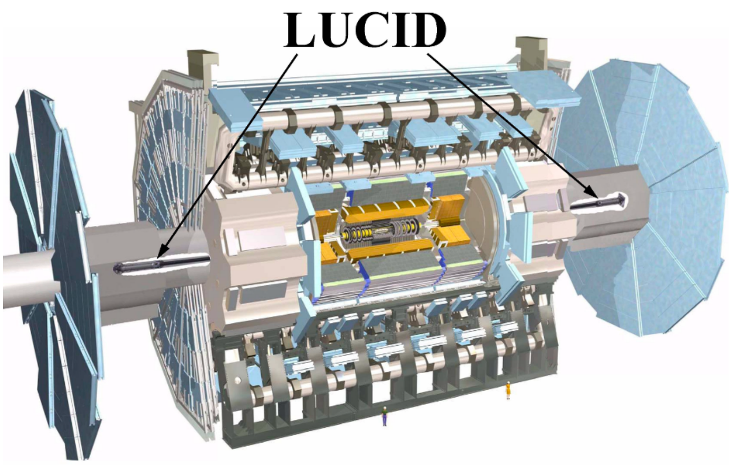

Figure 1: Current Location of the LUCID detector within ATLAS

This proximity exposes photomultiplier tubes to intense radiation, resulting in degradation of performance and the need for replacement. As the Large Hadron Collider prepares for its third long shutdown, the LUCID detector will undergo an upgrade to accommodate the demands of high luminosity.

The upgraded LUCID 3 detector will feature multiple sub-detectors to maximize redundancy and reliability. One of them will feature radiation-hard quartz fibers that generate Cherenkov light when ultra-relativistic particles enter them. The fibers allow for the light to be transmitted longer distances, enabling placement of the photomultiplier tubes in lower radiation zones. A prototype system using optical fibers is already installed and under testing within ATLAS.

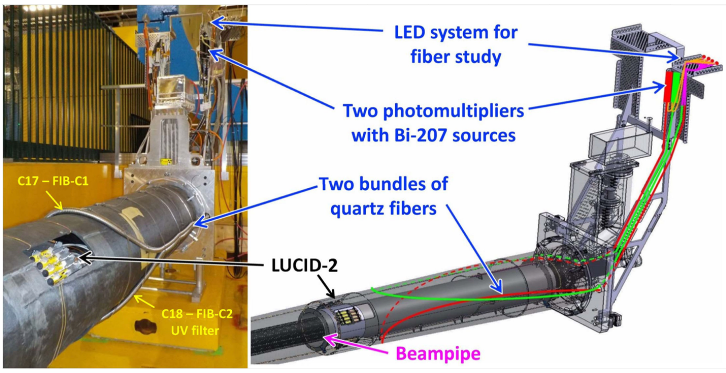

Figure 2: Current Prototype Under Testing

The goal of this project was to conduct benchmark testing of fiber transmission before irradiation. The central research question was how different fiber types perform across a range of wavelengths relevant to Cherenkov light prior to any radiation exposure. This will inform decisions about which fibers are most suitable for the final detector upgrade.

2 Experimental Methods

2.1 Fiber Types

Eleven fibers were tested, covering five different types of fiber. The main variables of interest are the numerical apertures and material make-up of the fibers. The fiber materials tested included UV, UVNS, UVNSS, and UVSRC. These materials tested are designed for deep UV transmission. The numerical apertures were varied using apertures of .12, .22, and .28. Each variation and its impact on transmission will be evaluated post-radiation.

2.2 Preparing Fibers

After the fibers are cut to the desired length, they are fitted with a ferrule to allow the connection of the fiber to an SMA adapter. After the ferrule has been attached, the fibers must be polished in order for the transmission of light through the fiber to be even. This process uses a fiber microscope and includes two stages of polishing. Figure 3 shows a fiber before polishing. Rough edges are still visible, preventing uniform light transmission across the surface.

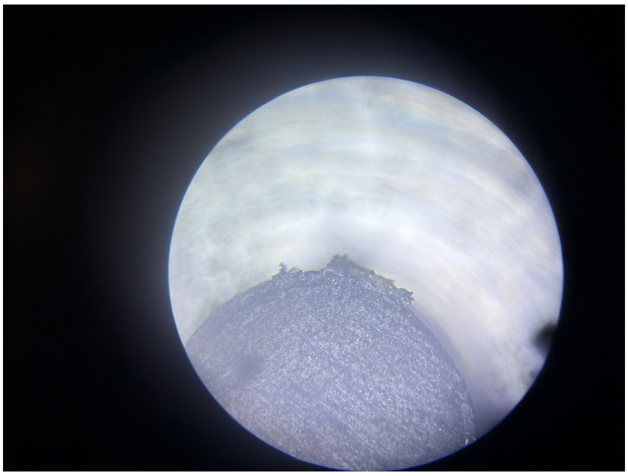

Figure 3: Fiber Before Polishing

Figure 4 is the fiber after it has been polished with a five-micron grit sandpaper. This stage leaves the fiber flush with the ferrule, but it still has deep scratches across its surface. The scratches could still affect the quality of the data, so it requires further polishing.

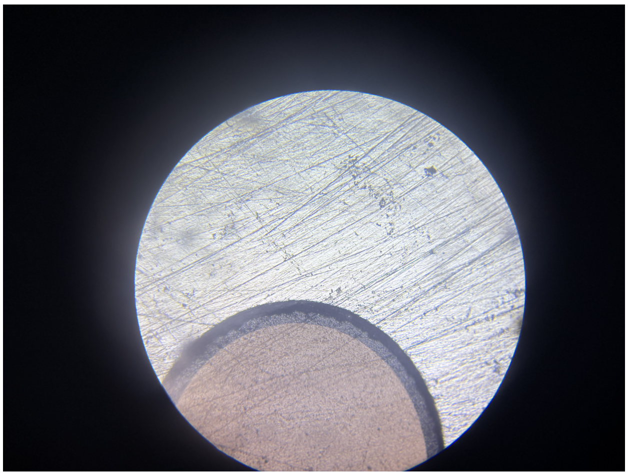

Figure 4: Fiber Polished with Five Micron Grit Paper

Figure 5 is the fiber after it has been polished with a one-micron grit sandpaper. This eliminates all of the visible scratches from the surface and allows for an even transmission of light across its surface.

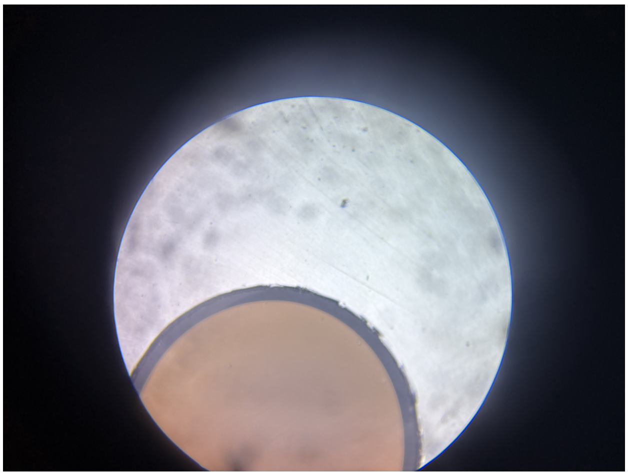

Figure 5: Fiber Completely Polished

2.3 Measurement Setup

A measurement system was constructed to assess the light transmission properties of each fiber. Four light-emitting diodes (LEDs) were used as the light sources, covering wavelengths from 280 nanometers to 625 nanometers. A four-wire cable connected the arduino board to the circuit. This circuit was built to reduce the number of cables and allow selective powering of the LEDs. Each power supply arduino pin is associated with a UV LED and a component of the RGB array. Because the polarities of the LED pair will always be opposite, the ground and power supply can be inverted, selectively powering only one in the pair. This allows three power supply pins to control six LEDs.

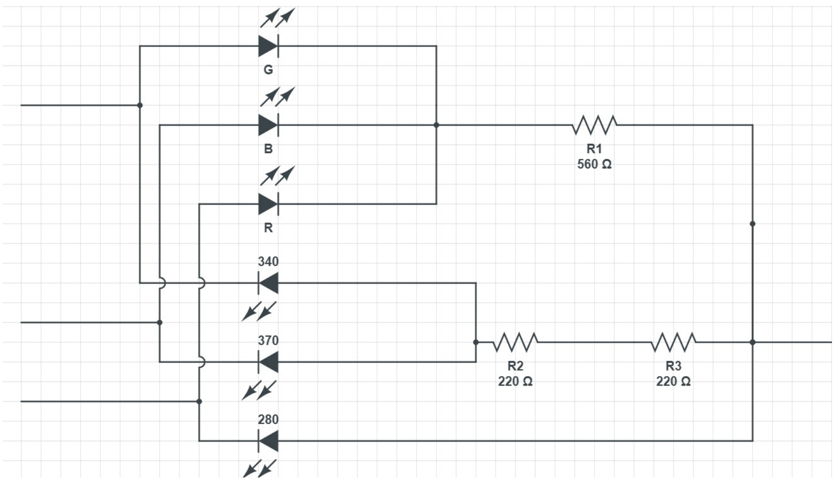

Figure 6: The Circuit Controlling the LEDs

The light from the LEDs was then routed into a custom-built light-sealed black box containing a distribution network. This network split the light from four sources into three outputs, allowing connection to two fibers simultaneously. Although testing two fibers simultaneously is possible, only two PIN diodes were available, so one fiber was tested at a time. Before the light can be measured by the devices, a pin-diode has to be used to convert the light intensity to current. The light intensity before going through the fiber was measured using a sourcemeter, and the light transmitted through the fiber was measured with a picoammeter.

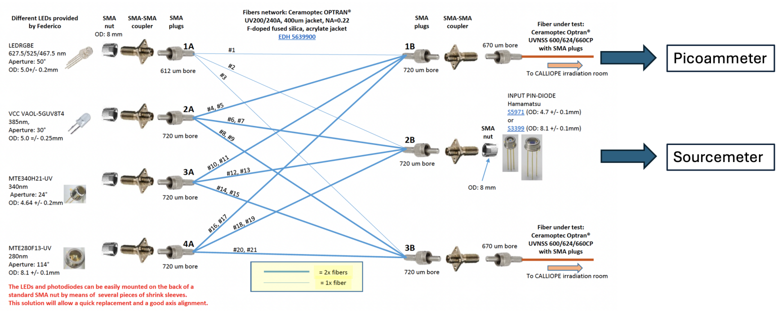

Figure 7: LED Distribution Network

A picoammeter is being used to test the light transmittance through the fiber because it is more sensitive to lower current values than the sourcemeter. This sensitivity will be necessary once the fibers have been irradiated.

2.4 Wavelength Selection

The wavelength range used in the experiment was selected based on the spectrum of Cherenkov radiation, which is most intense in the ultraviolet and blue regions. The UV region is the most important aspect of this project. The blue LED will be an important landmark to have, but the transmittance in the blue should not decrease significantly post-irradiation. Green and red wavelengths were also measured, though these were included primarily for completeness and will have a marginal effect on final conclusions.

2.5 Measurement Procedure

After the fiber was connected to the LED distribution system, a Python script automated the cycling of all LEDs and collected corresponding current values. At the end of each cycle, a background measurement (with all LEDs off) was recorded to quantify noise and subtract it from the previous measurements in the cycle.

Each PIN diode has an associated quantum efficiency, meaning that only a portion of the incident light is converted into measurable current. Differences in these efficiencies between diodes can introduce errors into the measurements. To correct for this, each fiber was measured in two separate runs. During the second run, the positions of the PIN diodes were swapped. This produced four data sets: two from the initial configuration, and two more after swapping the diodes. The measurements yield four equations:

$$I_1 = Q_a \cdot I_a \tag{1}$$
$$I_2 = Q_b \cdot I_b \tag{2}$$
$$I_3 = Q_b \cdot I_a \tag{3}$$
$$I_4 = Q_a \cdot I_b \tag{4}$$

I_a is the incident light being transmitted through the fiber, and I_b is the light being transmitted directly from the LED. Q_a and Q_b are the quantum efficiencies of the two pin diodes. I_1 and I_3 are the currents read by the picoammeter. I_2 and I_4 are the currents read by the sourcemeter. Applying the four resulting equations, the ratio of the averaged picoammeter currents to the averaged sourcemeter currents effectively cancels out the contribution of the pin diodes quantum efficiency.

$$\frac{I_1 + I_3}{I_2 + I_4} = \frac{I_a}{I_b} \tag{5}$$

3 Results

3.1 Fiber Transmission

The main metric of interest was the ratio of picoammeter to sourcemeter current. This ratio represents the relative transmission efficiency of each fiber.

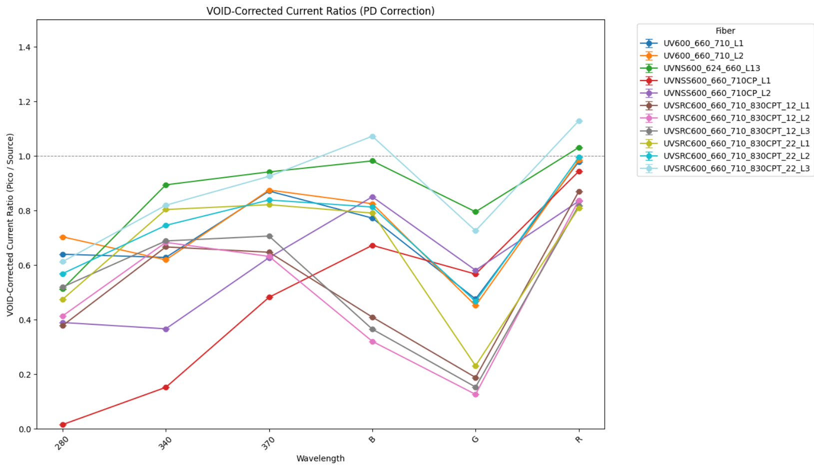

Figure 8: Run One of Pin Diode Corrected Data

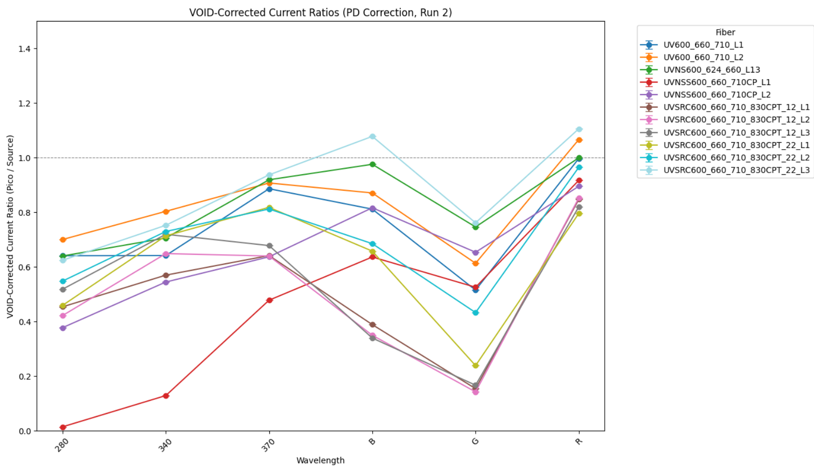

Figure 9: Run Two of Pin Diode Corrected Data

The transmission data remained relatively consistent across both runs. Using the data from Figure 1 and Figure 2, a benchmark can be established for post-irradiation testing.

3.2 Anomalous Fiber Behavior

The fiber UVNSS600_660_710CP_L1 displayed significantly lower transmission in the ultraviolet, a behavior that mimics that of irradiated fibers. This anomaly was consistent across both runs. Its counterpart fiber, UVNSS600_660_710CP_L2, was also lower than expected.

3.3 Data Corrections

The data points before corrections displayed large percentage differences between runs, especially in the 280 nanometer category.

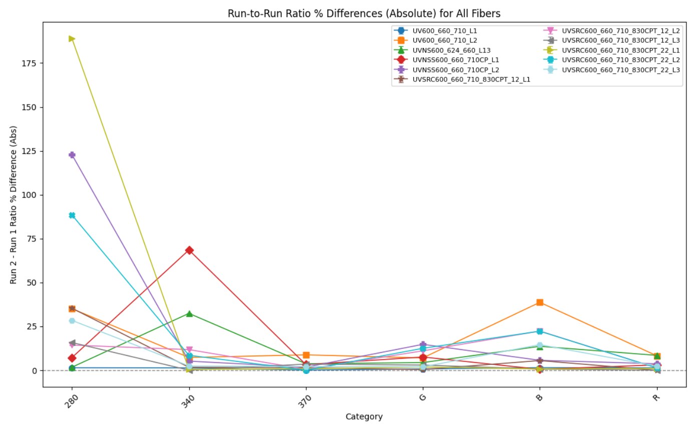

Figure 10: Percent Difference Between Runs of Uncorrected Data

To investigate the large differences across all of the wavelengths, the stability of the current was plotted for all of the fibers. Figure 11 is an example of a stability plot for one fiber.

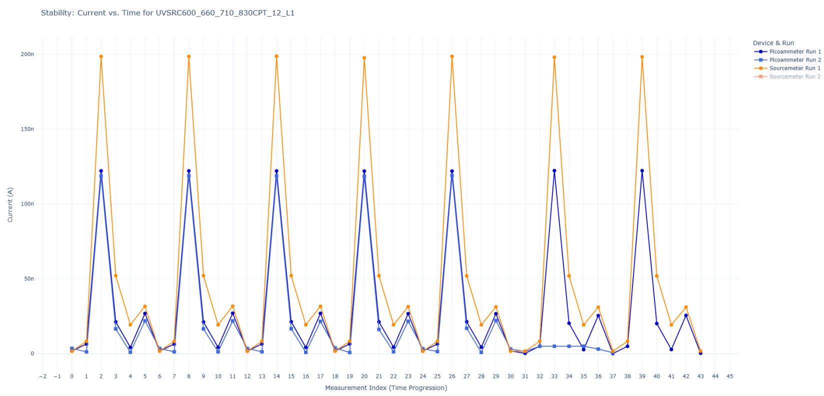

Figure 11: Plot of the Current vs. Time

Figure 11 shows significant instability in the current. Around the 32 index on the time axis, a significant drop can be observed in the readings from the picoammeter. This behavior suggests a potential issue with circuit connectivity. It appears that the values were consistently the same as the background noise previously read in the run. This suggests the LEDs had shut off for this duration of time. Fibers with this issue were ran once more. This improved the percentage differences between runs, but the issue in the 280 nanometer category remained. So, it was tested if the higher voltage requirements for the 280-nanometer LED was creating the issue. The LED requires 7 volts, but the arduino board only provides five volts. An external power supply was used to supply the correct voltage to the LED. Figure 12 is the new percentage difference between runs after the corrections had been made.

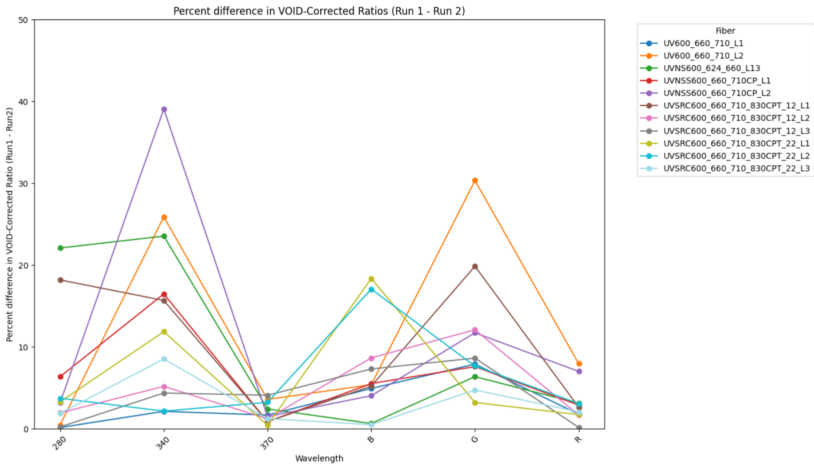

Figure 12: Percent Difference Between Runs of Corrected Data

Significant improvements can be seen in the data with these corrections. This improvement can especially be seen in the 280-nanometer wavelength. This strongly suggests the issue was the proper voltage not being supplied. There are inconsistencies in the blue and Green LED's. This is likely due to them not being centered in the RGB array. This creates coupling inconsistencies from run to run. Because the main transmission drop post-radiation will be in the UV range, this inconsistency will not be significant enough to affect post-radiation conclusions. There are still outliers in the 340-nanometer data that need to be investigated.

3.4 External Transmission Test for the 340 nanometer LED

To examine the outliers in the 340-nanometer range, an independent test was performed using a black box, two photomultiplier tubes and a pulsed 340-nanometer LED. The LED was connected to a three fiber splitter. Two paths sent light directly from the LED. The third path went through the fiber under test. The direct signal and the fiber-transmitted signal appeared as distinct yellow peaks in the recorded waveform. The blue peak is the second PMT receiving light from the LED.

Figure 13: Example Waveform with the PMTs

By taking multiple measurements where the orientation of the splitter is changed, light distribution inequality can be removed. Then the amplitude of the three peaks can be used to find the transmission of the fiber. The following table compares the ratios found using the PMTs to the ratios found in run 1 and run 2 using the original setup:

Fiber	PMT	LED 1	LED 2	% Diff 1	% Diff 2
UVNS600/624/660/L13	0.7885	0.8944	0.7059	12.58	11.06
UVNSS600/660/710/L2	0.7253	0.3666	0.5447	65.70	28.43
UV-SRC 600 NA=0.22	0.8111	0.8039	0.7525	0.89	7.50
UV-SRC 600 NA=0.12	0.3408	0.6669	0.5699	64.71	50.30
UV 600 NA=0.22	0.7813	0.6282	0.8036	21.73	2.81

Table 1: Comparison of PMT and LED testing results across fiber types. Percent differences are calculated between PMT and each LED run.

The PMT showed similar transmission of UV light through all of the fibers. The one exception is the fiber UV-SRC 600 NA=0.12 which showed a significant drop in transmission when tested with the PMT's. When comparing this data with the original set-up data, significant variation is still observed among a couple of fibers. The fiber UV-SRC 600 NA=0.12 shows a significant percentage difference when compared with run 1 and run 2. This suggests smaller numerical apertures may be more prone to coupling inconsistencies. The second fiber of interest, UVNSS 600/660/710/L2 NA = 0.22, showed significant improvements in transmission when tested with the PMT. The value seen using the PMT is closer to what is expected.

4 Discussion and Conclusions

All pre-irradiation benchmarking of candidate fibers for the LUCID upgrade has been completed, providing a baseline for interpreting changes after radiation exposure. These results, corrected for PIN diode efficiency and supported by external testing, will serve as a benchmark for post-irradiation comparison. Notably, smaller numerical aperture fibers appear more susceptible to coupling issues, and the UVNSS fiber pair showed significantly lower transmission in LED testing, both warrant further investigation. The current setup does have limitations. The RGB LED array produces unequal light intensity across outputs, particularly for the blue and green channels, introducing additional variance between runs. Future improvements will focus on addressing these limitations and improving the measurement process. A new circuit will be developed to test fibers in series without multiple picoammeters or manual reconnections, reducing the risk of damage or contamination. Additionally, an upgraded LED distribution network will enable simultaneous testing of up to five fibers with the three LEDs.

This work contributes to ensuring that the upgraded LUCID detector is both reliable and optimized for the high-luminosity era of the Large Hadron Collider, with the infrastructure now in place to complete post-irradiation evaluations and finalize fiber selection.